

## Supporting Information for

### Molecular level insight into the differential oxidase and oxygenase reactivities of *de novo* *Due Ferri* proteins

Rae Ana Snyder, Susan E. Butch, Amanda J. Reig, William F. DeGrado, and Edward I. Solomon

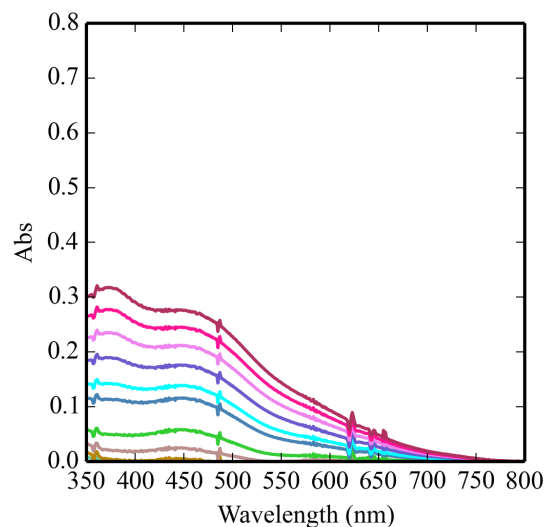


Figure S1: 4-aminophenol oxidation over 10 min by 3His-G4DFsc(Mut3) without *m*-phenylenediamine. Substrate was added anaerobically before the protein solution was reacted with O<sub>2</sub> saturated buffer.

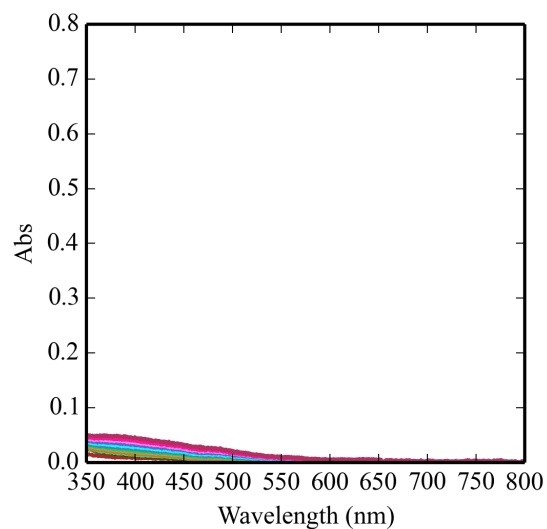


Figure S2: 4-aminophenol auto-oxidation without the DF protein and with *m*-phenylenediamine at pH 7 over 10 min.

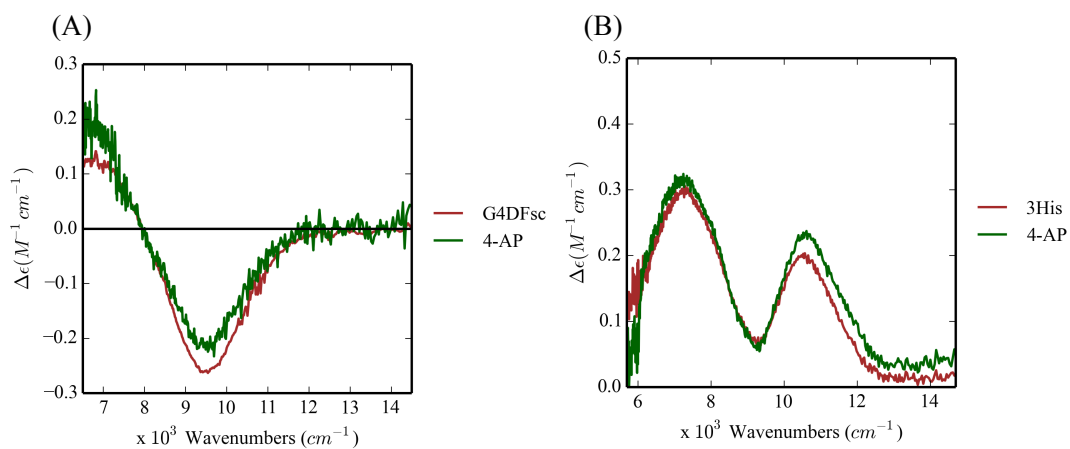


Figure S3 The effect of 4-aminophenol (4-AP) on the CD of Fe(II)Fe(II) state for (A) G4DFsc and (B) 3His-G4DFsc(Mut3).

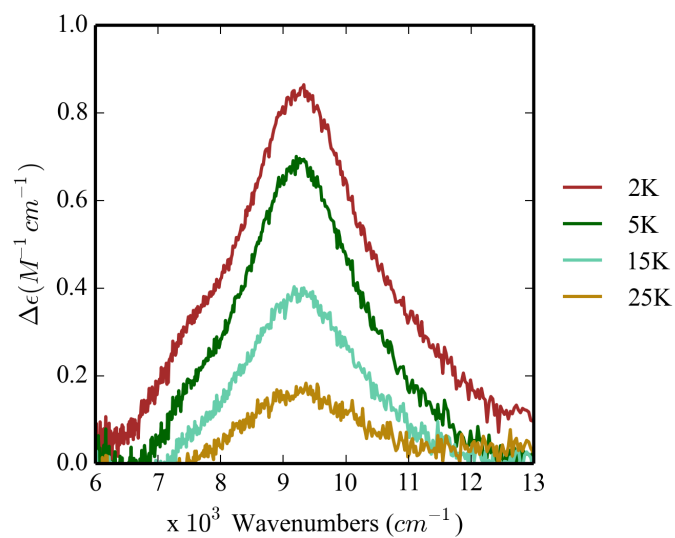


Figure S4: Temperature variation of the MCD spectra of G4DFsc in the presence of 4-AP, showing the C-term behavior of the new feature.

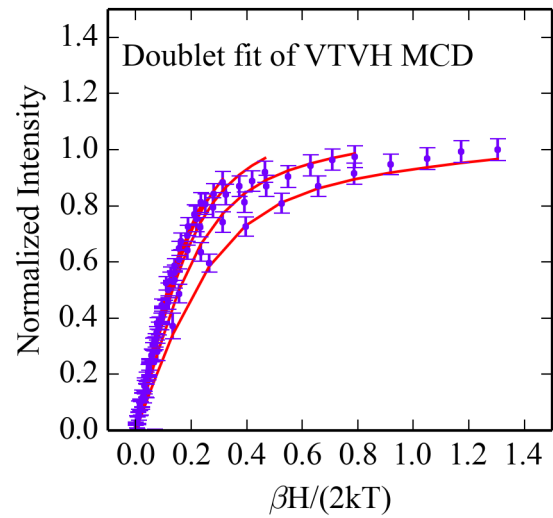


Figure S5: Doublet fit of the VTVH MCD data for G4DFsc in the presence of 4-aminophenol.

Table S1: Doublet fit and spin-Hamiltonian parameters for G4DFsc and 3His-G4DFsc(Mut3)

		G4DFsc	3His	G4DFsc+4-AP	3His+4-AP
Doublet Fit Parameters	$g_{  GS}(\text{cm}^{-1})$	4.0	8.0	8.0	8.0
	$\delta_{GS}(\text{cm}^{-1})$	3.0	4.0	1.2	1.2
	$A_{tot}$	1.1	2.0	1.5	1.7
	B-term (% $A_{tot}$ )	6.7	0.5	-3.2	-0.8
	Energy ( $\text{cm}^{-1}$ )	0.0	0.0	0.0	0.0
	$g_{  ES1}(\text{cm}^{-1})$	--	4.0	4.0	4.0
	$\delta_{ES1}(\text{cm}^{-1})$	--	6.0	6.0	6.0
	$A_{tot}$	--	3.4	3.5	1.4
	B-term (% $A_{tot}$ )	2.61 (arb)	0.2	3.2	3.5
	Energy ( $\text{cm}^{-1}$ )	4.8	3.0	1.7	1.7
	$g_{  ES2}(\text{cm}^{-1})$	--	--	12.0	12.0
	$\delta_{ES2}(\text{cm}^{-1})$	--	--	0.0	0.0
	$A_{tot}$	--	--	1.2	6.1
	B-term (% $A_{tot}$ )	--	--	-12.0	-6.0
Energy ( $\text{cm}^{-1}$ )	--	--	19.2	19.2	
Spin Hamiltonian Parameters	$-J(\text{cm}^{-1})$	3-4	1-3	< 1	< 1
	$D_1(\text{cm}^{-1})$	5-10	10-15	5-15	5-15
	$(E/D)_1$	0.33	0.33	0.33	0.33
	$D_2(\text{cm}^{-1})$	-7 to -14	-10 to -15	-5 to -15	-5 to -15
	$(E/D)_2$	0.15	0.33	0.33	0.33

The VTVH MCD data for both 3His-G4DFsc(Mut3)+4-AP (Figure 7 (B)) and G4DFsc+4-AP (Figure S5) were fit with three doublets where the ground sublevel has a  $g_{||GS} = 8.0$  with  $\delta_{GS} = 1.2 \text{ cm}^{-1}$  the first excited sublevel (at  $1 \text{ cm}^{-1}$ ) has  $g_{||ES1} = 4.0$  with  $\delta_{ES1} = 6.0 \text{ cm}^{-1}$  and the next excited sublevel (at  $19 \text{ cm}^{-1}$ ) has  $g_{||ES1} = 12.0$  with  $\delta_{ES1} = 0.0 \text{ cm}^{-1}$  (Table S1). This VTVH MCD behavior for the substrate bound forms is similar to that of the 3His form without substrate but with quantitative differences that arise from a decrease in the excited state sublevel from  $3 \text{ cm}^{-1}$  (in the unbound form) to  $1.7 \text{ cm}^{-1}$  (in +4-AP forms). A ground state with  $g_{||}$  of 8 indicates that it corresponds to a sublevel with  $|M_S| = 2$  and a first excited state with  $g_{||}$  of 4 requires it to have an  $|M_S| = 1$ .

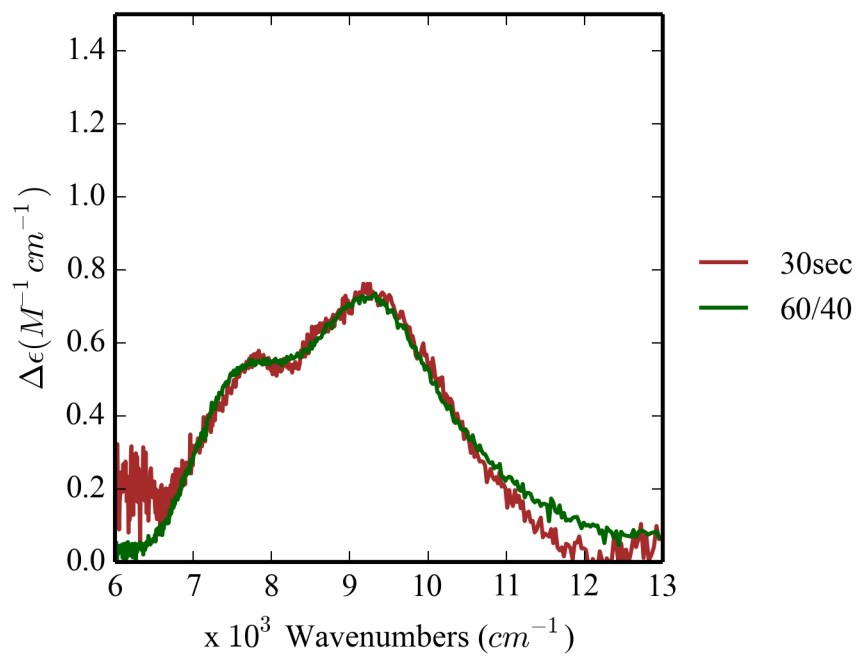


Figure S6: The composition of the intermediate MCD spectrum of G4DFsc when 4-aminophenol is added. Red is the intermediate spectrum obtained after waiting 30 s before freezing the MCD sample. Green is a composition of 0.6 x G4DFsc+4-AP and 0.4 x G4DFsc spectra.

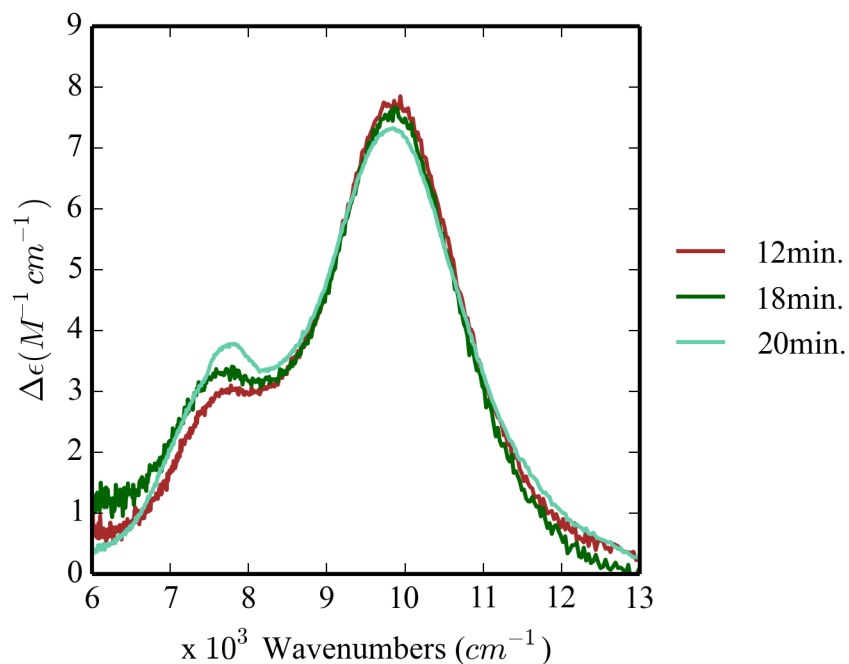


Figure S7: MCD spectra of 3His-G4DFsc(Mut3) in the presence of 4-aminophenol at longer time intervals.

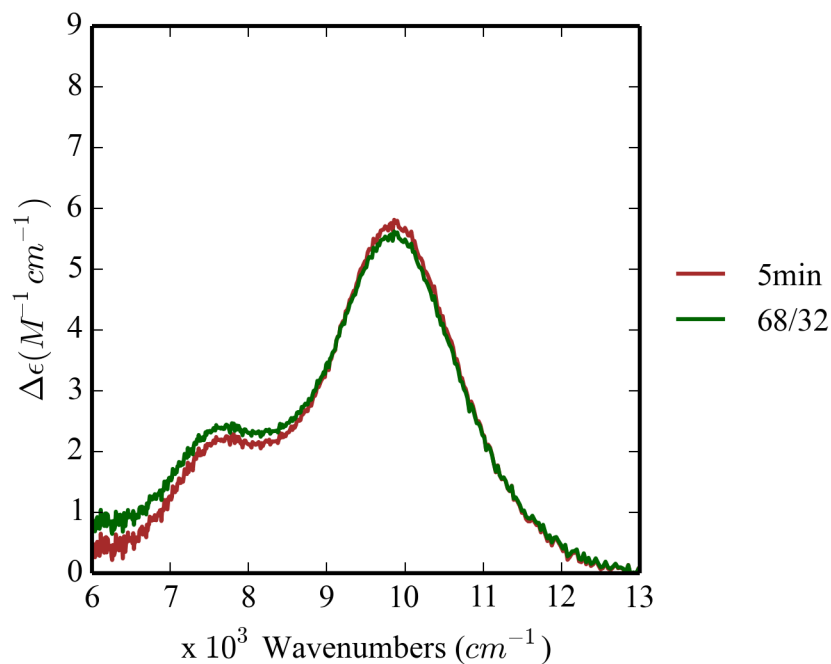


Figure S8: The composition of the intermediate MCD spectrum of 3His-G4DFsc(Mut3) when 4-aminophenol is added. Red is the intermediate spectrum obtained after waiting 5 min before freezing the MCD sample. Green is a composition of 0.68 x 3His-G4DFsc(Mut3)+4-AP (from 18 min spectrum) and 0.32 x 3His-G4DFsc(Mut3) spectra.

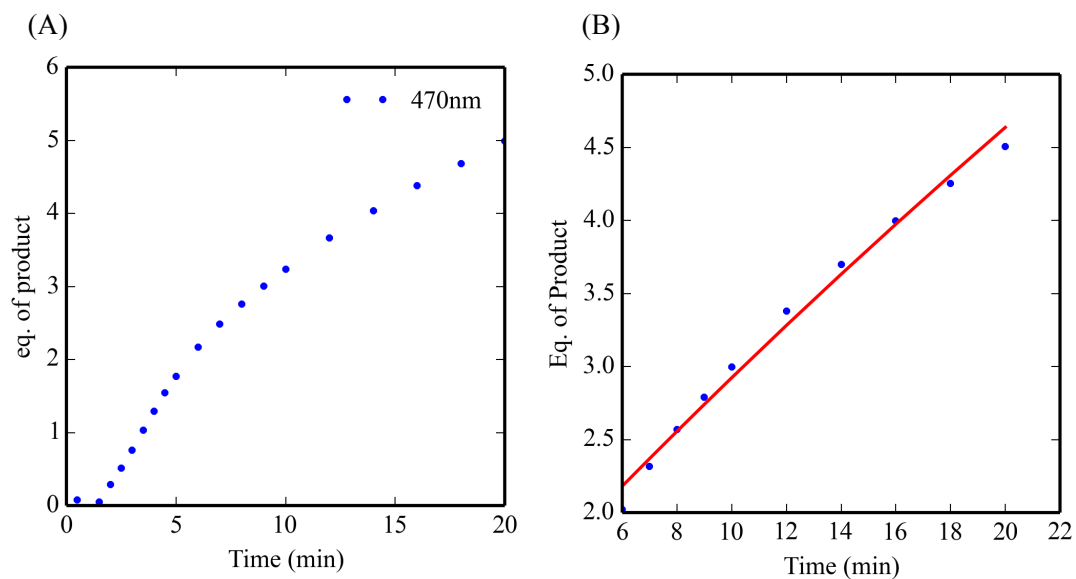


Figure S9: Kinetic trace for the 470 nm feature of 3His-G4DFsc+4-AP reacted with O<sub>2</sub> saturated buffer in the presence of *m*-phenylenediamine. (A) full kinetic trace and (B) kinetic trace with fit during turnover conditions. This aniline dye is a coupled product, and thus, the initial kinetics should include the rate of coupling benzoquinone imine to *m*-phenylenediamine.

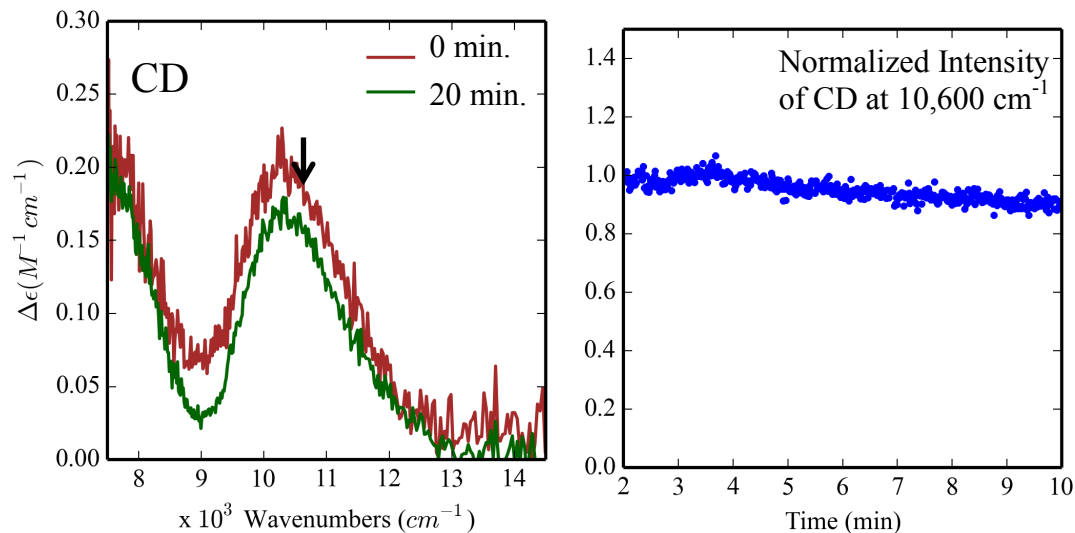


Figure S10: The decay of the bifurcated CD features during the 4-aminophenol oxidation reaction. CD of 3His-G4DFsc(Mut3)+4-AP before (red) and after (green) addition of  $O_2$  saturated buffer (right). The time course of the normalized intensity of the CD feature at 10,600  $cm^{-1}$  (left) over 10 min. CD data collected at 4  $^{\circ}C$  in the presence of  $\sim 15$ -fold excess substrate ( $\sim 0.25$  mM protein).

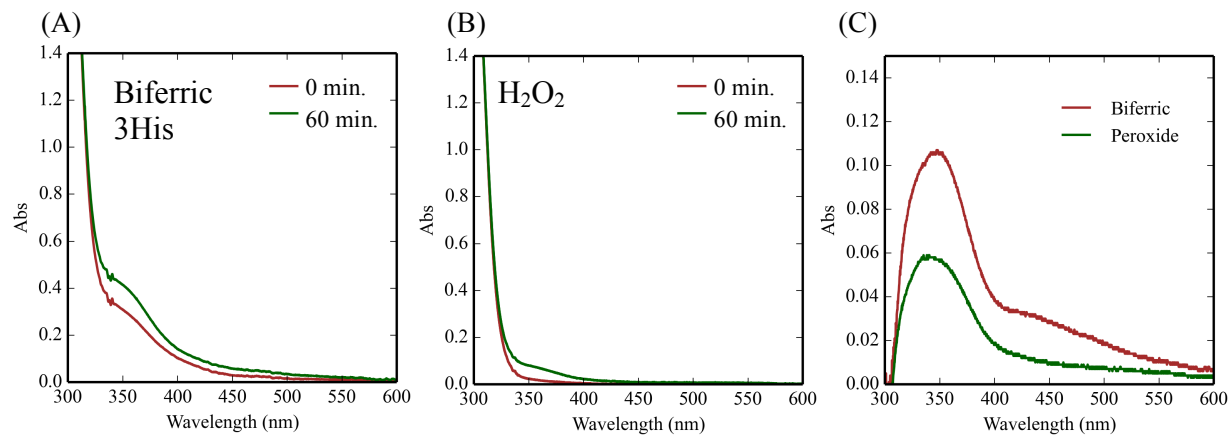


Figure S11: UV-Vis absorption spectra of *p*-anisidine oxidation by  $H_2O_2$ . (A) Biferric-3His-G4DFsc(Mut3) (150  $\mu M$ ) without buffer exchanging after  $O_2$  reaction. (B)  $H_2O_2$  addition to *p*-anisidine. (C) Difference spectra between 0 and 60 min in (A) and (B).



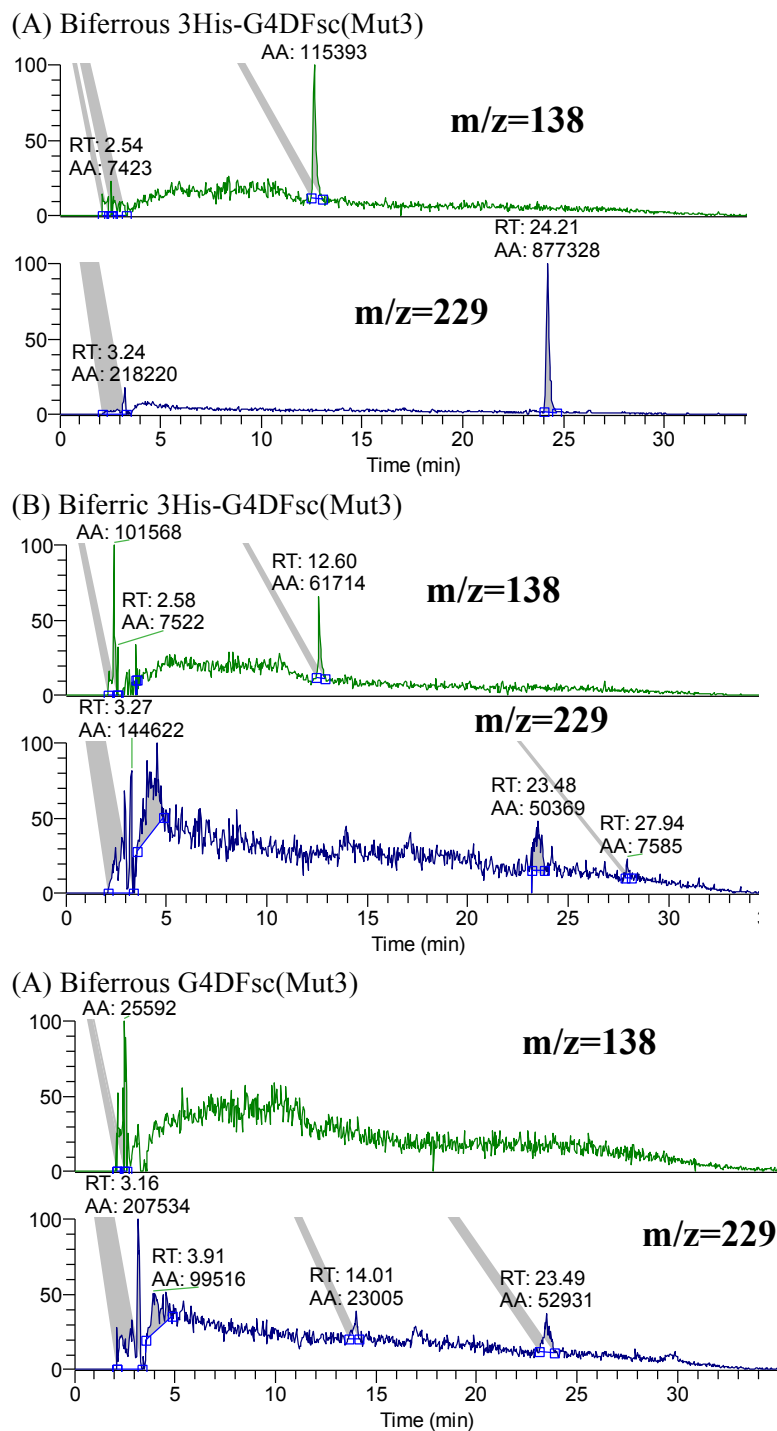


Figure S12: LCMS chromatographs of the *p*-anisidine oxidation for (A) anaerobic addition of *p*-anisidine to biferrous 3His-G4DFsc(Mut3) followed by the addition of O<sub>2</sub> saturated buffer, (B) simultaneous addition of *p*-anisidine and O<sub>2</sub> saturated buffer to 3His-G4DFsc(Mut3). (C) anaerobic addition of *p*-anisidine to biferrous G4DFsc followed by addition of O<sub>2</sub> saturated buffer. Top is the  $m/z=138$  and bottom is the  $m/z=229$  ion extracted chromatographs associated with 4-nitroso-methoxybenzene and 4-methoxy-*N*-(4-nitrosophenyl)aniline.

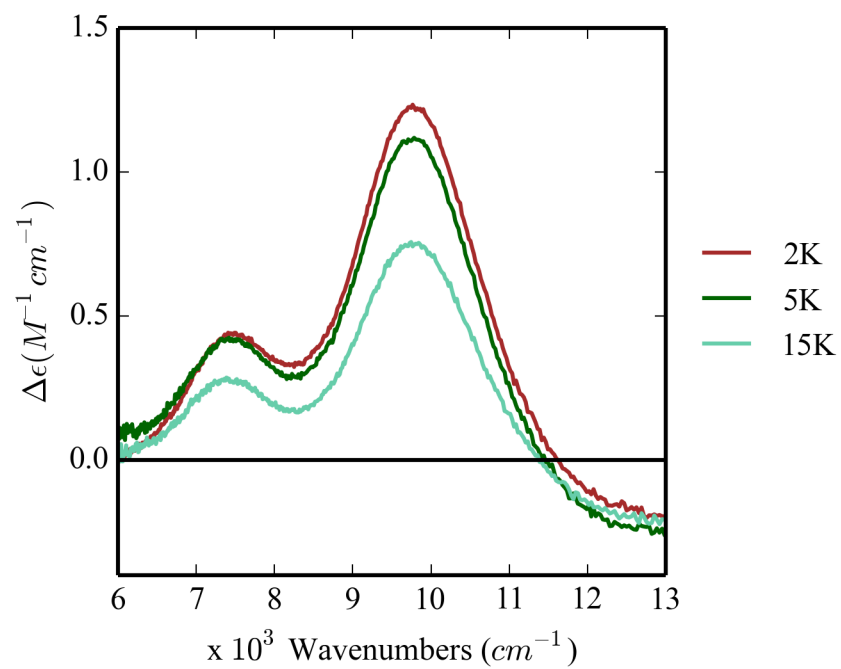


Figure S13: MCD spectra of 3His-G4DFsc+p-anisidine at variable temperatures.

Table S2: Doublet fit and spin Hamiltonian parameters for G4DFsc and 3His-G4DFsc(Mut3) in the presence of *p*-anisidine.

		G4DFsc	3His-G4DFsc(Mut3)
Doublet Fit Parameters	$g_{  GS}(\text{cm}^{-1})$	8.0	4.0
	$\delta_{GS}(\text{cm}^{-1})$	2.0	3.0
	$A_{tot}$	1.8	1.0
	B-term (% $A_{tot}$ )	0.6	-21.0
	Energy ( $\text{cm}^{-1}$ )	0.0	0.0
	$g_{  ES1}(\text{cm}^{-1})$	4.0	8.0
	$\delta_{ES1}(\text{cm}^{-1})$	3.0	1.0
	$A_{tot}$	2.5	4.7
	B-term (% $A_{tot}$ )	2.0	-1.4
	Energy ( $\text{cm}^{-1}$ )	1.7	0.7
	$g_{  ES2}(\text{cm}^{-1})$	--	--
	$\delta_{ES2}(\text{cm}^{-1})$	--	--
	$A_{tot}$	--	--
	B-term (% $A_{tot}$ )	--	-0.1 (arb.)
Energy ( $\text{cm}^{-1}$ )	--	14.0	
Spin Hamiltonian Parameters	$-J(\text{cm}^{-1})$	< 2	2-3
	$D_1(\text{cm}^{-1})$	5-15	5-10
	$(E/D)_1$	0.33	0.33
	$D_2(\text{cm}^{-1})$	-5 to -15	-5 to -10
	$(E/D)_2$	0.33	0.33

For G4DFsc+P-AN, the VTVH MCD data (Figure 14 (A)) were fit using the doublet model to two spin sublevels: a  $g_{||GS} = 8.0$  ( $|M_S| = 2$ ) ground sublevel with a  $\delta_{GS} = 2.0 \text{ cm}^{-1}$  and an  $g_{||ES} = 4.0$  ( $|M_S| = 1$ ) excited sublevel with  $\delta_{ES} = 3.0 \text{ cm}^{-1}$  at  $1.7 \text{ cm}^{-1}$  (Table S2). This fit indicates that the addition of substrate has changed the ground sublevel from  $|M_S| = 1$  (for G4DFsc) to an  $|M_S| = 2$  (for G4DFsc+P-AN). This fit indicates that the addition of substrate has changed the ground sublevel from  $|M_S| = 1$  (for G4DFsc) to an  $|M_S| = 2$  (for G4DFsc+P-AN). This change in ground sublevel represents altered spin-Hamiltonian parameter values (in eq. 1). Since the energies of the ferrous  $d \rightarrow d$  transitions in the NIR CD and MCD spectra were only minimally perturbed,

the ZFS of the associated Fe(II) center should not have significantly changed. Therefore, this ground sublevel difference reflects a decrease in the antiferromagnetic coupling between the two Fe(II) centers (as represented by the orange arrow on the correlation diagram in Figure S19).

For 3His-G4DFsc(Mut3)+P-AN, the VTVH MCD data (Figure 14 (B)) were fit with three spin sublevels: a  $g_{||GS} = 4.0$  ( $|M_S| = 1$ ) ground state with  $\delta_{GS} = 3.0 \text{ cm}^{-1}$ , a  $g_{||ES1} = 8.0$  ( $|M_S| = 2$ ) first excited state with  $\delta_{ES1} = 1.0 \text{ cm}^{-1}$  at  $0.7 \text{ cm}^{-1}$  and a second excited state that is a singlet at  $14 \text{ cm}^{-1}$  (Table S2). The ferrous  $d \rightarrow d$  transitions of the 3His form in the NIR CD and MCD spectra also do not significantly change, and thus, the shift in the ground state from  $|M_S| = 2$  to  $|M_S| = 1$  upon the addition of P-AN to 3His-G4DFsc(Mut3) reflects a slight increase in the magnitude of the antiferromagnetic coupling (blue arrow in Figure S19) ( $-J \sim 2\text{-}3 \text{ cm}^{-1}$  3His-G4DFsc(Mut3)+P-AN with substrate, and  $1\text{-}2 \text{ cm}^{-1}$  without) (Table 2).

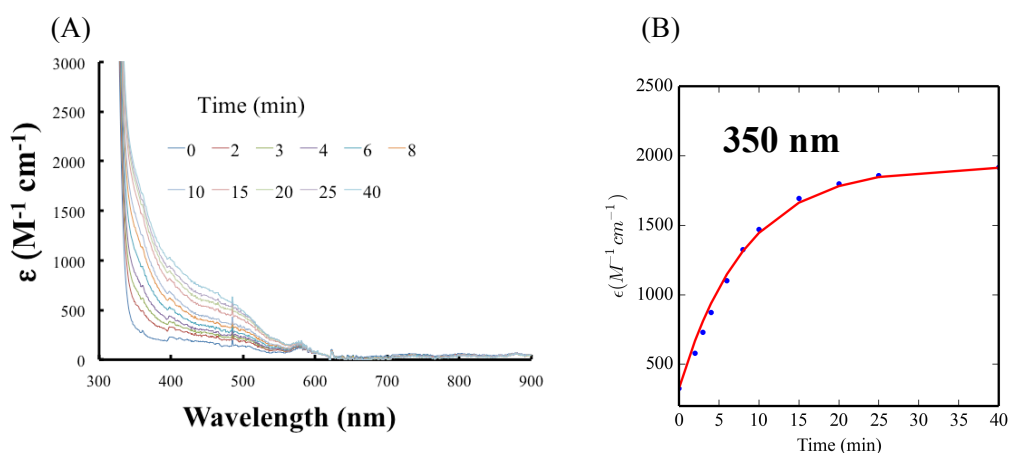


Figure S14:  $O_2$  reactivity of G4DFsc+P-AN. (A) Abs spectra following the addition of  $O_2$  saturated buffer to G4DFsc+4-AP. (B) Kinetic trace of 350 nm (data in blue, fit ( $k_1 = 0.002 \text{ s}^{-1}$ ) in red).

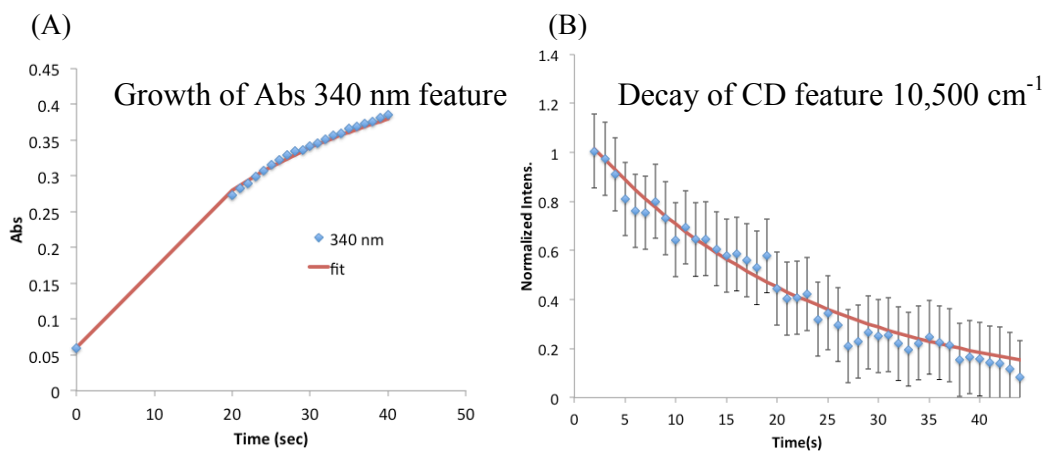


Figure S15: Pre-steady state kinetic traces of O<sub>2</sub> reactivity for 3His-G4DFsc(Mut3)+P-AN . (A) Absorption kinetic trace of the formation of the nitroso product at 340 nm with fit that is a simple A to B model ( $1-\exp(-k_1t)$ ), where  $k_1 = 0.045 \text{ s}^{-1}$ . (B) CD kinetic trace of the biferrous feature at 10,500  $\text{cm}^{-1}$  fit with a simple decay (red) where  $k_1 = 0.045 \text{ s}^{-1}$ .

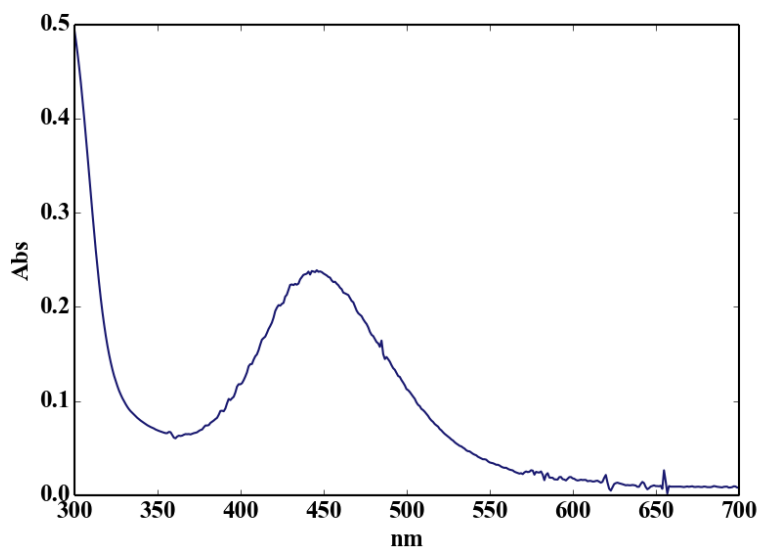


Figure S16: UV-Vis absorption spectrum of *p*-anisidine reaction with 3His-G4DFsc(Mut3) and O<sub>2</sub> after 48 hours. Reaction mixture contained 250  $\mu\text{M}$  protein with 20-fold excess *p*-anisidine that was diluted by 250-fold before data collection. Concentrations: 1  $\mu\text{M}$  of protein, 9  $\mu\text{M}$  of the indoaniline dye (9 eq. of product).

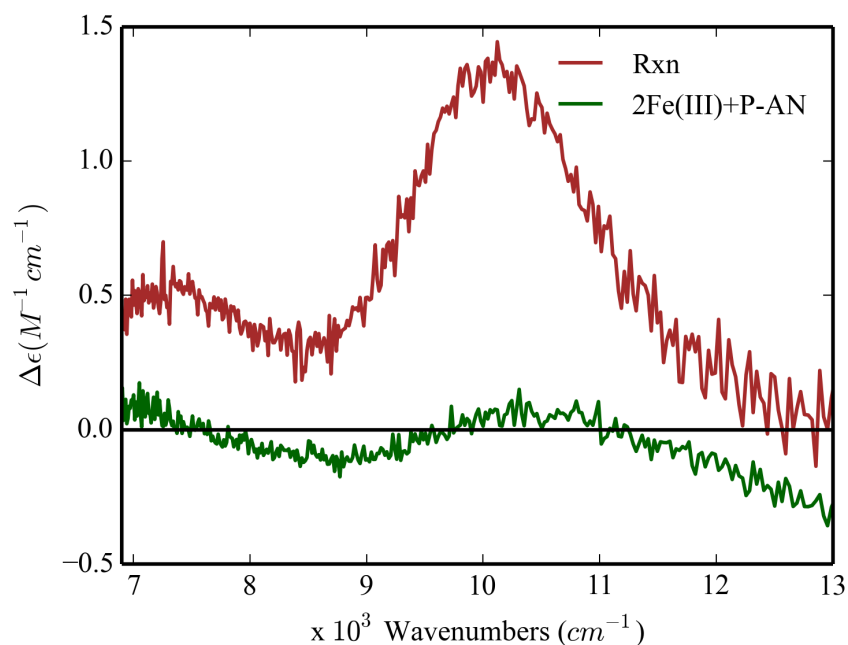


Figure S17: MCD of different reaction conditions for *p*-anisidine and 3His-G4DFsc(Mut3). MCD spectrum collected after allowing biferrous 3His-G4DFsc(Mut3)+P-AN to react with O<sub>2</sub> saturated buffer for 60 min and then degassing sample (red) and MCD spectrum collected of biferrous form of 3His-G4DFsc(Mut3) after addition of *p*-anisidine (2+ hours) (green).

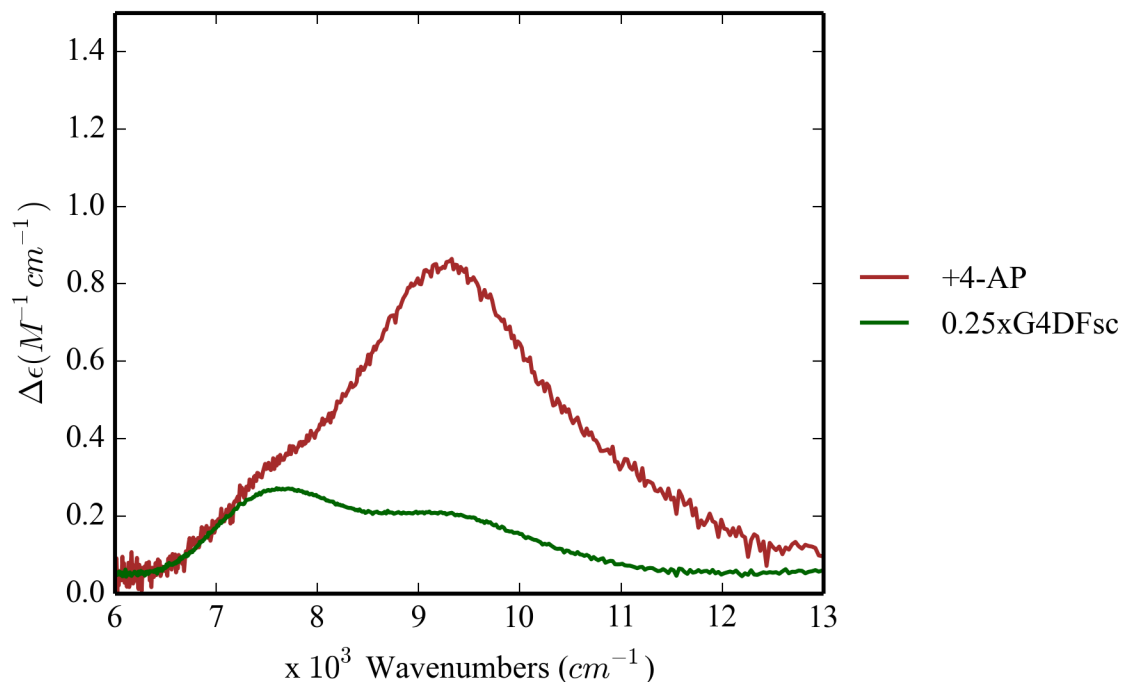


Figure S18: Based on the MCD spectra of G4DFsc+4-AP and G4DFsc, unbound species present in reaction mixture is less than 25%. In addition, the sustained presence of the biferrous 3His NIR CD band during turnover indicates that enzyme is likely fully saturated with substrate above (3 mM) as any unbound species would be oxidized and not participate in turnover.

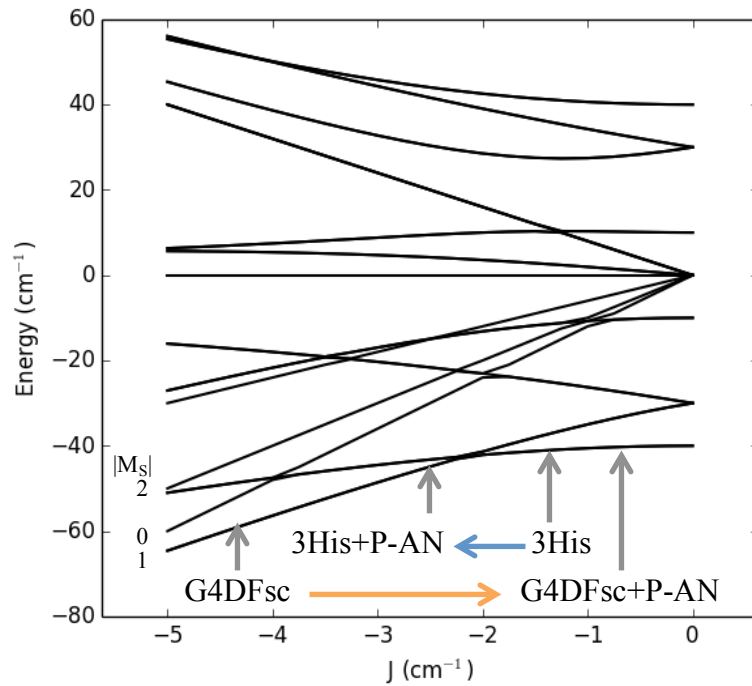


Figure S19: Correlation energy diagram for antiferromagnetic coupling for oppositely signed axial ZFS parameters. For this diagram,  $D_1 = -10$  and  $D_2 = 10 \text{ cm}^{-1}$  and  $E/D = 0$  (for simplicity). Grey arrows indicate the relative positions in magnetic coupling for G4DFsc and 3His-G4DFsc(Mut3) (3His) without and with (+P-AN) *p*-anisidine. Orange and blue arrows indicate the direction of change in magnetic coupling upon *p*-anisidine addition for G4DFsc and 3His.

## Supporting Materials and Methods

*LCMS of product formation.* *p*-anisidine was anaerobically added to biferrous protein and incubated for ~20 min. The sample was then placed in an anaerobic UV-Vis absorption cell. O<sub>2</sub> saturated buffer was added to the protein solution (dilution of protein by 1/2) at 4 °C and rapidly mixed with a pipet. Final concentrations of samples contained 100 μM of protein and 1 mM of substrate in 150 mM MOPS/150 mM NaCl buffer at pH 7. The samples were left for several days at 4 °C. The 200 μL samples were diluted 1:10 fold with water and passed through a Polaris C18 250x2.1 mm column with 4 μm particles (Agilent) and detected by UV absorption at 214 nm. Gradient provided below:

Time (min)	A% (1% Formic acid in water)	B% (1% Formic Acid in acetonitrile)	Flow rate (ml/min)
0	100	0	0.25
4	100	0	0.25
30	5	95	0.25
31	5	95	0.25
31.1	100	0	0.25
35	100	0	0.25

*H<sub>2</sub>O<sub>2</sub> oxidation of p-anisidine:* A solution of buffer (150 mM MOPS/150 mM NaCl at pH 7) was prepared with 1 mM *p*-anisidine. H<sub>2</sub>O<sub>2</sub> was added (100 μM) prior to collecting the UV-Vis absorption spectrum at 0 and 60 min.

*Non-buffer exchanged biferric oxygenase assay:* O<sub>2</sub>-saturated buffer was added to biferrous protein solution (dilution of protein by 1/2) at 4 °C and mixed with a pipet. This solution was allowed to react for 1 hour at 4 °C. *p*-anisidine was then added to the solution and the UV-Vis absorption spectrum was collected at 0 and 60 min. Final concentrations for protein and substrate were 100 μM and 1 mM.

*O<sub>2</sub> reactivity of G4DFsc with p-anisidine.* *p*-anisidine was anaerobically added to biferrous protein and incubated for ~20 min. The sample was then placed in an anaerobic UV-Vis absorption cell. O<sub>2</sub> saturated buffer was added to the protein solution (dilution of protein by 1/2) at 20 °C, rapidly mixed with a pipet and spectra were collected every 10 seconds for the first minute, every minute for the first 10 min., and then every 10 min afterward. After O<sub>2</sub> saturated buffer (prepared by sparging O<sub>2</sub> gas into buffer in a closed vessel for ~15 min. at 20 °C) addition, the sample was maintained under aerobic conditions. Final concentration for protein and substrate were 100 μM and 1 mM.

*Turnover of p-anisidine oxygenase by 3His-G4DFsc(Mut3).* *p*-anisidine was anaerobically added to biferrous protein and incubated for ~20 min. O<sub>2</sub> containing buffer was added to the protein solution (dilution of protein by 1/2) at 20 °C. Final concentration for protein and substrate were 250 μM and 5 mM after addition of O<sub>2</sub> containing buffer. The solution was left at 20 °C for 48 hours under aerobic conditions.